Physiological, Biochemical, and Mathematical Studies of Micro-Aerobic Continuous Ethanol Fermentation by *Saccharomyces cerevisiae.* II: Intracellular Metabolite and Enzyme Assays at Steady State Chemostat Cultures

Ron Grosz* and Gregory Stephanopoulos
Department of Chemical Engineering, Massachusetts Institute of Technology, Cambridge, Massachusetts 02139

Accepted for publication June 4, 1990

Intracellular metabolite concentration and enzyme activity measurements were made to explain the new metabolic and growth phenomena seen in the micro-aerobic, continuous yeast cultures described in Part I. The results of these assays suggested mechanisms for the observed maximum in the specific ethanol productivity as a function of the oxygen feed rate, changing ATP yields, the effects of antifoam, and the sharp changes in the biomass concentration with small changes in the oxygenation. Measured were the intracellular concentrations of ATP, NADH, glucose 6-phosphate, pyruvate, glycerol, and ethanol, and the activities of hexokinase and alcohol dehydrogenase. Rate-limiting steps were identified by the accumulation of metabolites upstream and the depletion of metabolites downstream of the step.

A potential mechanism for the stimulation of fermentation with decreasing oxygenation was an activation of glucose transport by an accumulating intracellular ATP concentration. The inhibition of fermentation at yet lower oxygenation rates may have been caused by the continued accumulation of ATP to the point that the glycolytic kineses were inhibited. A mechanism for the changing ATP yields and intracellular ATP concentration proposed the existence of ATPases or ATP waste reactions stimulated by both oxygen and ATP. Antifoam had the effect of decreasing the resistance for glycerol transport out of the cell. The resulting stimulation of glycerol production and inhibition of ethanol production decreased the intracellular ATP content. Finally, intracellular ethanol was found not to accumulate to levels of higher than the extracellular concentration.

INTRODUCTION

In the first part of this series,[1] some unusual behaviors of micro-aerobic yeast metabolism were discussed. The steady-state specific ethanol productivity attained a sharp maximum as a function of the oxygenation rate. Specifically, in run 9, (Part 1, Fig. 1), the steady-state specific ethanol productivity increased by over 50% as the percent oxygen in the gas feed was reduced from 0.38 to 0.024%. When the oxygen feed was further reduced to 0.0058%, the specific ethanol productivity reversed its trend and decreased by over 50%. This confirmed a similar observation by Nishizawa et al.[2] that the specific ethanol productivity attained a maximum at 10 ppb dissolved oxygen.

In addition, in Part I, respiration rates were measured and shown to contribute negligibly to the overall ATP production in these oxygen-limited, glucose-repressed cultures. Therefore, the Crabtree and Pasteur effects,[3] mechanisms by which fermentation is influenced by changing respiration, could not have participated in the changing fermentation rates of this study.

In this article, the mechanism behind the maximum specific ethanol productivity is explored. The intracellular concentrations of ethanol, glycerol, pyruvate, glucose 6-phosphate, APT, and NADH, and the activities of hexokinase (EC 2.7.1.1) and alcohol dehydrogenase (EC 1.1.1.1) were assayed during the steady states of runs 9 and 10 of Part I. The metabolite assays aided in the identification of crossover points[4] or rate limiting steps in glycolysis that caused the changes in the metabolic rate. Cofactor and enzyme activity measurements aided in identifying the cause of the rate limitation.

The changes in the specific ethanol production occurred at a constant specific growth rate, since the chemostat dilution rate remained constant, and only the oxygen addition rate was manipulated. Therefore, it was calculated in Part I that the ATP yield or energetic efficiency of biosynthesis changed significantly along with the fermentation parameters. In this article, intracellular ATP measurements are presented along with

* Present address: E. I. DuPont de Nemours & Co., Experimental Station, Engineering Technology Laboratory, Wilmington, Delaware 19880

Biotechnology and Bioengineering, Vol. 36, Pp. 1020–1029 (1990)

CCC 0006-3592/90/01001020–010$04.00

mechanisms known from the literature in an attempt of explaining the changing ATP yield.

High concentrations of the silicone polymer Antifoam B was found, in Part I, to have numerous effects on the chemostat culture. The specific ethanol production rates were lower and the specific glycerol production rates higher than in the corresponding cultures with lower antifoam concentrations (Part I, Figs. 1, 2, and 11). In addition, the steady-state biomass concentration underwent hysteresis, characterized by sudden drops in the biomass concentration when the oxygen addition rate dropped below a critical value. (Part I, Fig. 9). Intracellular glycerol assays in this study revealed an influence of high antifoam on the resistance to glycerol export from the cell and could account for the altered metabolic pattern. In addition, intracellular ATP concentration measurements documented the energetic consequences of the metabolic changes caused by high antifoam levels, and also suggested a possible cause for the hysteresis in the biomass concentration.

Finally, it is shown that intracellular ethanol does not accumulate above extracellular levels, agreeing with the observations of Dasari et al.,[5] but disagreeing with the results of other investigators.[6,7] The difference may lie in the difference in the assay method. The method used here avoids sampling delays and accounts for any accumulation of extracellular ethanol during the sampling period which would otherwise be falsely attributed to intracellular ethanol.

MATERIALS AND METHODS

Cultivation of Cells

S. cerevisiae cells were grown in continuous culture in a glucose, yeast-extract-based medium and under oxygen limitation. Specifically, several steady-state cultures of runs 9 and 10 of the first article[1] provided the cells for the enzyme and the metabolite assays; exact culture conditions can be found there.

Preparation of Cell-Free Extracts for Enzyme Assays

Fermentor fluid (5–25 mL), depending on the cell density, was sampled over crushed ice and centrifuged for 10 min at $2 \times 10^4 g$ and 4°C. The pellet was resuspended in ice-cold 1*M* Tris buffer, pH 7.5, and recentrifuged. The pellet was resuspended in 5 mL of the same Tris buffer and the suspension added to 4 mL of 0.45–0.5-mm glass beads in a 12-mL culture tube. The suspension was homogenized in a Braun MSK homogenizer with the temperature controlled at 4°C for 2.25 min at 4000 rpm. The homogenate was filtered through a coarse fritted buchner funnel to remove the glass beads. The beads were washed twice with 1 mL of the ice-cold Tris buffer, and the washes added to the filtered homogenate. Two to three extracts were prepared for enzyme activity assay at each chemostat steady state. The optimal breakup time was chosen to effect greater than 90% breakup of the cells by three measures: total protein release, fumarase activity release, and broken to unbroken population counts made with a Coulter counter.[8]

Cell Extract Preparations for ATP, Glucose 6-Phosphate, Intracellular Pyruvate, and Intracellular Glycerol Assays

The extraction method described in this section was used for the assay of all intracellular metabolites except NADH and intracellular ethanol. The reason for these exclusions is given in the description of the alternate extraction method.

Fermentor fluid (5–25 mL) was loaded into a syringe and rapidly pushed through a 0.45-μm filter housed in a syringe filtration unit. The filter and the yeast paste were quickly recovered and immediately placed into 5 mL of ice-cold 6% perchloric acid. The submerged filter was agitated to hasten the permeation of the yeast paste by the extractant. Less than 15 s elapsed between the sampling and the contacting of the yeast with the perchloric acid. The extract was placed in an ice bath for 30 min and then neutralized dropwise with 3*M* $KHCO_3$. Three extracts were prepared for metabolite assay at each fermentor steady state. The development process for this protocol is described below.

The greatest challenge in developing an extraction protocol arises from the extremely rapid (of the order of 1 s) turnover rate of the intracellular metabolite pool.[9,10] Sampling and inactivation need not occur in one second, but in a time scale sufficiently short that the concentrations of the limiting substrate in the cells' environment do not change significantly.

Direct sampling of the fermentor liquid into −20°C, 35% perchloric acid, as performed by Weibel et al.[11] was initially attempted. However, this extraction method failed with all assays except ATP because it provided no means for separating the cells from the supernatant. Extracellular pyruvate (up to 0.1 g/L) and glycerol masked the intracellular levels. In addition, fluorophores in the yeast extract medium interfered with the fluorimetric assays of glucose 6-phosphate and pyruvate (to be described). The ATP assay succeeded with this extraction protocol because it is an intracellular compound and because the culture supernatant did not interfere with the bioluminescence assay. Thus, the ATP assay enabled the comparison between this and the other assay methods tested.

To eliminate interference from extracellular metabolites and fluorophores, the method of Franco et al.[10] was attempted. The fermentor sample was mixed with percholoric acid precooled to −20°C in a syringe. The mixture was immediately pushed with a syringe plunger through a 0.5 μm pore size syringe filter. The cell pellet, substantially free of extracellular medium, was then

recovered. Franco et al. claimed that no intracellular metabolites leak out of the cell for at least 180 s of perchloric acid contact within which the sample could be filtered. However, under the culture conditions in which the yeast cells were grown in this study, this method was found to be unsuitable. When the ATP assay was used to compare this method to the method of Weibel et al.,[11] it was found that 73% of the ATP leaked out of the cell and passed through the filter.

To circumvent the problem with the other extraction methods, the culture fluid was rapidly filtered before contacting perchloric acid. In this way, the fluorophores in the medium which interfered with the glucose 6-phosphate and intracellular pyruvate measurements were eliminated. In addition, this extraction method yielded the same intracellular ATP concentration as the method of Weibel et al.,[11] so that the 15-s delay between sampling and extraction did not cause an altered intracellular metabolite profile. Two unique circumstances of these experiments might explain this fact. First, there was, by design, a high residual glucose concentration (greater than 20 g/L) in the fermentor. It can be calculated that less than 5% of the glucose in the medium was consumed during the sampling, so that the high degree of saturation of the glucose transporter was not significantly changed. Second, the high glucose concentration and the micro-aerobic conditions significantly repressed the respiratory enzymes. Thus, exposure to atmospheric oxygen during sampling had minimal consequences on the overall metabolism of these respiratory incompetent cells.

There was yet one complication with this extraction method for the intracellular pyruvate and glycerol measurements. Since the yeast paste was not washed prior to immersion into the extractant, some extracellular pyruvate and glycerol were introduced into the extract from the interstitial fluid of the yeast paste. A correction was made to the intracellular measurements after calculating this interstitial volume and measuring the extracellular concentrations. An upcoming section is devoted to this calculation.

Cell Extract Preparation for NADH and Intracellular Ethanol Measurements

This alkaline extraction was developed because NADH is rapidly destroyed by acid. It was also used for intracellular ethanol measurements because degradation products in the perchloric acid extract coeluted with ethanol in the HPLC method used for ethanol determination.

Fermentor fluid (5–15 mL) was sampled and syringe filtered. Immediately, the cell paste and filter paper were placed in 2 mL of 1*N* NaOH at 60°C. Two milliliters of 0.3 g/L copper sulfate was added to the mixture. Heating in the water bath continued for 1 min, and the sample was submerged in an ice bath. The pH of the extract was reduced to 8.5–9 with 3% acetic acid. Three extracts were prepared for each steady state.

This extraction method was a modification of that of Polakis and Bartley.[12] When their method was applied to the samples of this study, externally added NAD^+ was completely converted to NADH, indicating that some dehydrogenases had not been deactivated. It was found that addition of copper sulfate in the present procedure prevented the nucleotide interconversion. In testing this method, external addition of NAD, NADPH, and NADP did not alter the NADH measurement.[8] Also, externally added NADH was quantitatively recovered.

As with the intracellular pyruvate and glycerol measurements, extracellular ethanol carried into the extract from the interstitial fluid of the yeast paste had to be deducted to yield only the intracellular ethanol content. The method of calculation is presented below.

Calculation of Intracellular Metabolite Concentrations when Extracellular Metabolites are Present

Pyruvate, glycerol, and ethanol are present both inside and outside the cell, so that measurement of only the intracellular content is complicated. In the extraction protocol for these metabolites, cells are filtered but not washed prior to extraction with NaOH or perchloric acid. Therefore, some of the metabolite in the extract is of extracellular origin, being introduced from the extracellular fluid in the interstitial spaces of the yeast paste. Washing the paste is not possible, as time delays and alteration of the cell environment is likely to change the intracellular metabolite levels. In addition, ethanol is thought to cross the cell membrane rapidly.[13]

In this section, a convenient method is introduced to account for the metabolites in the extract of extracellular origin. The intracellular component can be calculated by deducting the extracellular portion from the total. The terms of the equations to be presented are made clear by referring to the extraction protocols.

The method of calculation relies on two facts. First, the residual glucose concentration in the fermentor supernatant was higher than 20 g/L in all runs. Second, intracellular glucose concentrations are negligible.[14,15] Thus, the volume of the extracellular fluid in the extract can be estimated by the glucose concentration.

The total glucose content in the extract is given by:

$$G_{ext}[V_{per} + V_{neu} + V_{bio} + V_{int}] \quad (1)$$

where G_{ext} is the glucose concentration in extract (g/L); V_{per} is the volume of perchloric acid extraction solution (L); V_{neu} is the volume for extract neutralization (L); V_{bio} is the volume of biomass in yeast paste (L); and V_{int} is the interstitial volume in paste (L). In the case of the alkaline extraction, V_{per} is replaced by V_{NaOH}, the volume of the alkaline extraction solution. The total glucose content above is also equal to the amount of glucose carried into the extract, from the interstitial fluid, $G_{sup}V_{int}$, corrected by the amount taken up by the cells

during the sampling period, Δt (typically less than 5%):

$$G_{sup}V_{int} - \nu_g X V_{sam}\Delta t = G_{ext}[V_{per} + V_{neu} + V_{bio} + V_{int}] \quad (2)$$

where G_{sup} is the residual glucose concentration in fermentor supernatant (g/L); ν_g is the specific glucose uptake rate (g/g h); X is the biomass concentration in fermentor (g/L); V_{sam} is the sample volume (L); and Δt is the time delay from sampling to extraction (h). The above equation can be solved for the interstitial volume.

The intracellular concentration of component i can then be calculated by the equation:

$$C_i = \frac{C_{ext}[V_{per} + V_{neu} + V_{bio} + V_{int}] - \nu_i X V_{sam}\Delta t - C_{sup}V_{int}}{V_{sam}X} \quad (3)$$

where C_i is the intracellular concentration of i component (g/g dry wt); C_{ext} is the concentration of i in extract (g/L); ν_i is the specific production rate of i in fermentor (g/g h); and C_{sup} is the concentration in fermentor supernatant (g/L). Again, a correction has been made for the amount of metabolite excreted during the sampling period.

The typical calculation of the interstitial volume in the yeast paste ranged from 80 to 150 μL. This compares to a typical intracellular volume of 50 μL, based on 2 mL intracellular volume/g dry wt.[16] In the cases of ethanol and pyruvate, whose extracellular concentrations were comparable to the intracellular, the propagation of errors in these calculations was significant. Based on a 5% error in direct pyruvate and ethanol measurements, the calculated intracellular pyruvate concentration was accurate to 30% and the intracellular ethanol concentration to within 10 g/L of the reported values. However, these measurements still enabled the observation of general trends. In addition, this method is superior to any method that would involve washing the yeast paste before extraction, where the error introduced would be uncertain.

The intracellular glycerol concentration measurement was not subject to such large errors, because the intracelluar glycerol content was usually much greater than the extracellular one. The precision of this assay was $\pm 5\%$.

ATP Assay

The intracellular ATP from the perchloric acid extract was assayed with the firefly bioluminescence reaction governed by the following equation[17]:

$$\text{ATP} + \text{luciferin} + O_2 \xrightarrow{\text{luciferase}} \text{Oxyluciferin} + \text{AMP} + CO_2 + \text{light} \quad (4)$$

Luciferin was obtained from Sigma, and the luciferase from Boehringer Mannheim. The light emission was monitored in a fluorimeter with bioluminescence and total emission accessories. The temperature was maintained at 26°C. Pipetted into a cuvette were 500 μL buffer (Tris, 8.48 g/L; EDTA, 0.744 g/L, ph 7.7), 200 μL bovine serum albumin, 3 g/L; 200 μL magnesium acetate, 1.3 g/L; 40 μL luciferase; 0.167 mg/mL in 0.5M Tris buffer, pH 7.4; and 75 μL luciferin, 1 mg/mL in 0.1M Tris buffer, pH 7.4. The reaction was started by injecting 1 mL sample into the cuvette through a septum on the sample compartment.

The luminescence signal increased rapidly after injection, peaked, and gradually decayed for several minutes. The peak luminescence gave a linear calibration curve with ATP concentration in the relevant concentration ranges.[8] Two ATP measurements were made on each of the three extracts at each steady state. The measurements were within 10% of the mean.

Glucose 6-Phosphate Assay

The glucose 6-phosphate assay was based on the following reaction[11]:

$$\text{Glucose 6 - P} + \text{NADP} \xrightarrow[\text{Mg}]{\text{G6P dehydrogenase}} \text{NADPH} + \text{6 - P - gluconate} \quad (5)$$

The change in NADPH fluorescence was monitored at a 340-nm excitation, 460-nm emission wavelength pair in a fluorimeter. Reagents were obtained from Sigma. The reaction temperature was 26°C. Pipetted into the cuvette were 2.3 mL of 0.1M Tris buffer, pH 7.5; 100 μL NADP, 1 mg/mL in dilute HCl; 100 μL magnesium chloride, 30 g/L; and 500 μL sample. The reaction was started by the addition of 1 μL glucose 6-phosphate dehydrogenase preparation. Two to three glucose 6-phosphate measurements were made at each steady state. The variability was less than 10% of the mean.

Pyruvate Assay

The following reaction governs the pyruvate assays[11]:

$$\text{Pyruvate} + \text{NADH} \xrightarrow{\text{lactate dehydrogenase}} \text{lactate} + \text{NAD} \quad (6)$$

The disappearance of NADH was monitored fluorimetrically at the 340, 460-nm wavelength pair. The reaction temperature was 26°C. Pipetted into the cuvette were 2.9 mL Tris buffer, ph7.5; 60 μL of NADH, 0.1 mg/mL in 0.1M Tris, pH 9.5; and 20–100 μL sample. The reaction was initiated with the addition of 1 μL lactate dehydrogenase. A higher variability was seen in this assay compared to the other metabolite assays especially because of the correction for extracellular pyruvate in the extract. Six measurements were made per steady state, and these were mostly within 15% of the mean.

NADH Assay

The lactate dehydrogenase-based fluorometric assay was applied in the NADH assay.[9] Pipetted onto the cuvette were 2.4 mL 0.1*M* Tris, pH 7.5; 100 μL pyruvate, 0.25 g/L; and 500 μL sample. The reaction was initiated with 1 μL enzyme. Reproducibility of four to six repeat measurements was within 5%.

Hexokinase Assay

To assay hexokinase [EC 2.7.1.1] activity, its reaction was coupled with the glucose 6-phosphate dehydrogenase reaction[18]:

$$\text{Glucose} + \text{ATP} \xrightarrow{\text{hexokinase}} \text{glucose 6} - \text{phosphate} + \text{ADP} \quad (7)$$

$$\text{Glucose 6} - \text{P} + \text{NADP} \xrightarrow{\text{G6P dehydrogenase}} \text{6P} - \text{gluconate} + \text{NADPH} \quad (8)$$

The appearance of NADH absorbance at 340 nm was monitored in a spectrophotometer. Pipetted into the cuvette were 1.5 mL of 0.1*M* Tris buffer, pH 8.0; 1 mL glucose, 100 g/L in the above buffer; 200 μL magnesium chloride, 30 g/L, 200 μL NADP, 10 mg/mL in dilute acid; 100 μL ATP, 10 mg/mL in 0.1*M* citrate buffer, pH 8; and 2μL glucose 6-phosphate dehydrogenase solution. The reaction was initiated with 20 μL sample. Note the citrate buffer and a pH of 8 is essential for the ATP solution to avoid severe inhibition of the reaction.[19] Three repeat measurements per steady state were within 10% of the mean.

Alcohol [EC 1.1.1.1] Dehydrogenase Assay

The reaction governing the assay is[18]:

$$\text{Ethanol} + \text{NAD} \xrightarrow{\text{alcohol dehydrogenase}} \text{acetaldehyde} + \text{NADH} + \text{H}^+ \quad (9)$$

As usual, NADH absorbance is monitored at 340 nm. Pipetted into the cuvette were 2.3 mL of glycine, semicarbazide (pH = 9) buffer from Sigma, 200 μL NAD, 10 mg/mL in dilute acid, 200 μL $MgCl_2$, 30 g/L, and 20 μL sample. The reaction was initiated with 200 μL ethanol, 13% by volume. Three activity determinations were made per steady state with a precision of $\pm$10%.

RESULTS AND DISCUSSION

Maximum Specific Ethanol Productivity

As seen in run 9 (Part I, Fig. 1) and as presented by Nishizawa et al.,[2] the specific ethanol productivity was maximum at a low, but nonzero, oxygen feed percent. Intracellular enzyme and metabolite assays were performed during run 9 to elucidate the mechanism. For ease of presentation, the phenomenon is considered in two halves. The first half is the increasing specific ethanol productivity with decreasing oxygenation down to 0.024% feed oxygen. The second half is the inhibition of fermentation that occurred when the oxygen feed was reduced from 0.24 to 0.0058%.

The metabolic rates and intracellular parameters assayed in the region in which the specific ethanol productivity was increasing with decreasing oxygenation (the first half) are shown in Figure 1. In these graphs, the steady state at 0.0058% oxygen feed is omitted.

The intracellular metabolites, glucose 6-phosphate, intracellular pyruvate, and intracellular glycerol, all increased in concentration in parallel with the 50% increase in the specific ethanol productivity, as did the metabolic fluxes, the specific glucose uptake rate, glycerol production rate, and pyruvate production. In contrast, the hexokinase and alcohol dehydrogenase activities decreased or stayed almost constant with decreasing oxygen feed.

Since the glucose 6-phosphate and all metabolites downstream of it accumulated with the metabolic flux increase, some process upstream of glucose 6-phosphate, either glucose transport or hexokinase, must be rate limiting. The hexokinase activity was constant, so that any change in the reaction rate would have to be the result of modulation of this enzyme's activity by changing levels of the cofactor ATP. Figure 1 does indeed reveal that the intracellular ATP content doubled during the increased glycolytic flux. However, if one assumes an intracellular water volume of 2 mL/g dry wt,[16] the intracellular ATP concentration is more than an order of magnitude greater than the Michaelis-Menten constant of the enzyme.[20] In this range, the hexokinase activity cannot be influenced much.

A possible explanation for an increased transport activity is kinetics with respect to the extracellular glucose concentration. Plotted in Figure 2 is the specific glucose uptake rate as a function of the residual glucose concentration in the fermentor in runs 9 and 10. First, it must be noticed that changes in the transport rate are occurring at glucose concentrations much higher than the expected Michaelis–Menten half-saturation constants. Second, saturation kinetics is not obeyed, especially in run 10 in which the transport rate curves up more steeply at higher residual glucose concentrations. Finally, at low glucose concentrations in both runs 9 and 10, the transport rate and other metabolic rates do not vary significantly, even though the residual glucose concentration is different. Therefore, it is unlikely that saturation kinetics with respect to the glucose concentration is the sole cause of the changing glucose transport rate.

The intracellular ATP level may also influence the glucose transport rate. Spoerl et al.[20] theorized that the glucose transport enzyme is continually synthesized and degraded. As synthesis requires ATP, the glucose transport activity reflects the energetic state of the cell. Serrano and De La Fuente,[14] and Bisson and Fraenkel[21] also reported changes in the transporter properties in response to the metabolic state and aerobic adaptation

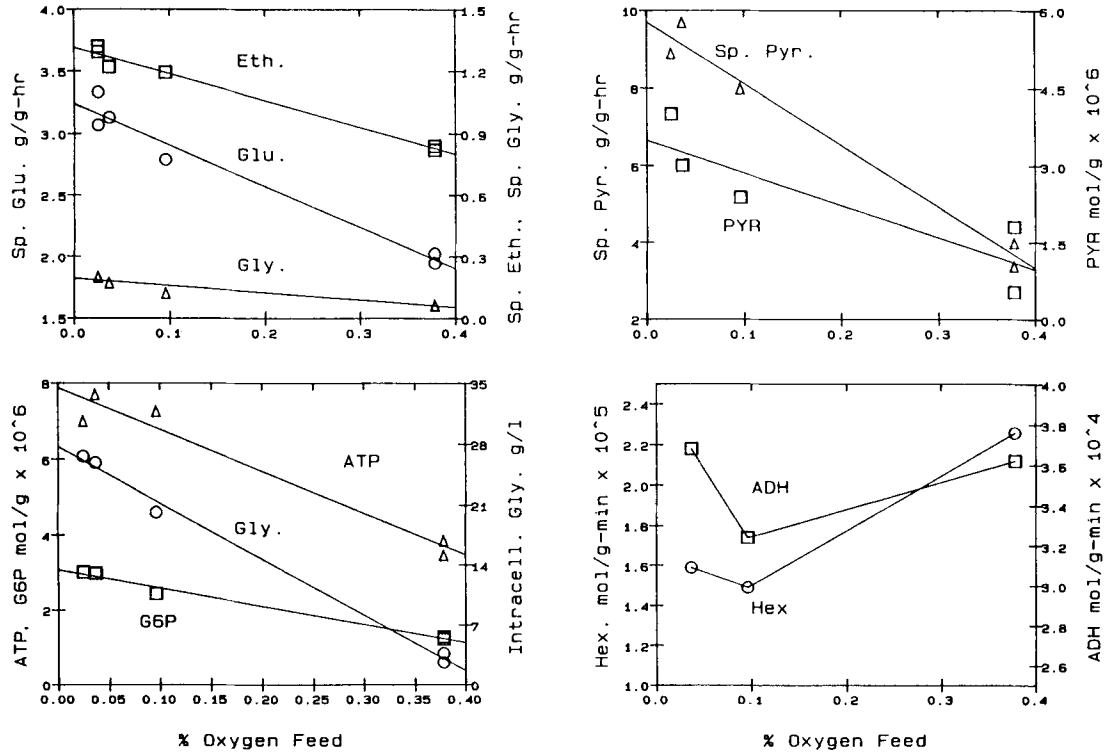

Figure 1. Intracellular enzyme and metabolite assays performed during steady states of run 9 in the region in which metabolic rates were increasing with decreasing oxygenation. Conditions for run 9 are given in Part I.

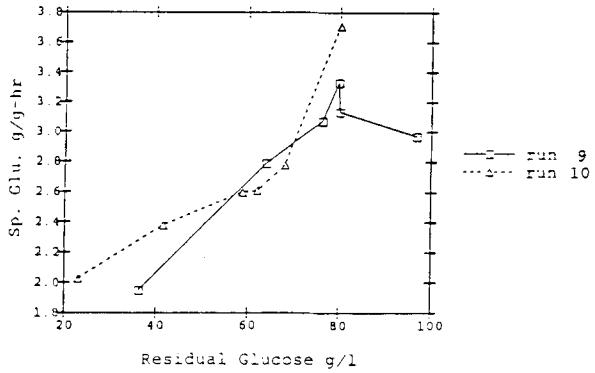

Figure 2. Glucose transport rate versus extracellular glucose concentration at steady state in runs 9 and 10.

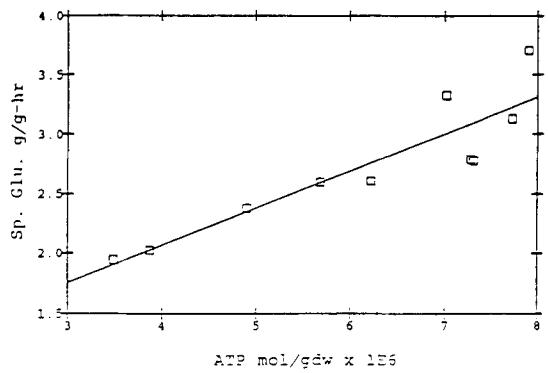

Figure 3. Glucose transport rate versus intracellular ATP concentration for runs 9 and 10.

of the cells. Plotted in Figure 3 is the specific glucose uptake rate versus the intracellular ATP concentration in runs 9 and 10. The trend suggests, but does not prove, that the glucose transport activity was influenced by ATP, and ultimately, this may have been the cause of the increased metabolic flux with the decreased oxygenation rate.

Attention is now turned to the second half of the phenomenon, the decreased specific ethanol productivity upon transition to the lowest oxygenation steady state of run 9. Shown in Figure 4 are the intracellular enzyme activity and metabolite assays performed during this transition. The data is similar to that of Figure 1, except that the steady state at 0.0058% oxygen feed in run 9 is added and that at 0.378% is omitted.

Clearly, there was a crossover point or rate limiting step causing this transition. Glucose 6-phosphate, intracellular glycerol, and NADH all accumulated, so that these metabolites must be upstream of the rate limiting step, or are influenced by conditions upstream of that step. Pyruvate and ethanol were depleted, so that these must have been downstream of the bottleneck.

With the aid of the results of Figure 4, a mechanism is proposed to account for the inhibition of ethanol production and the metabolite pattern. The mechanism is initiated by an accumulating ATP concentration upon transition to the lowest oxygen feed rate. This accumulation was actually measured and shown in Figure 4. An increased ATP concentration might also indicate an increased ATP-to-ADP ratio, making conditions subop-

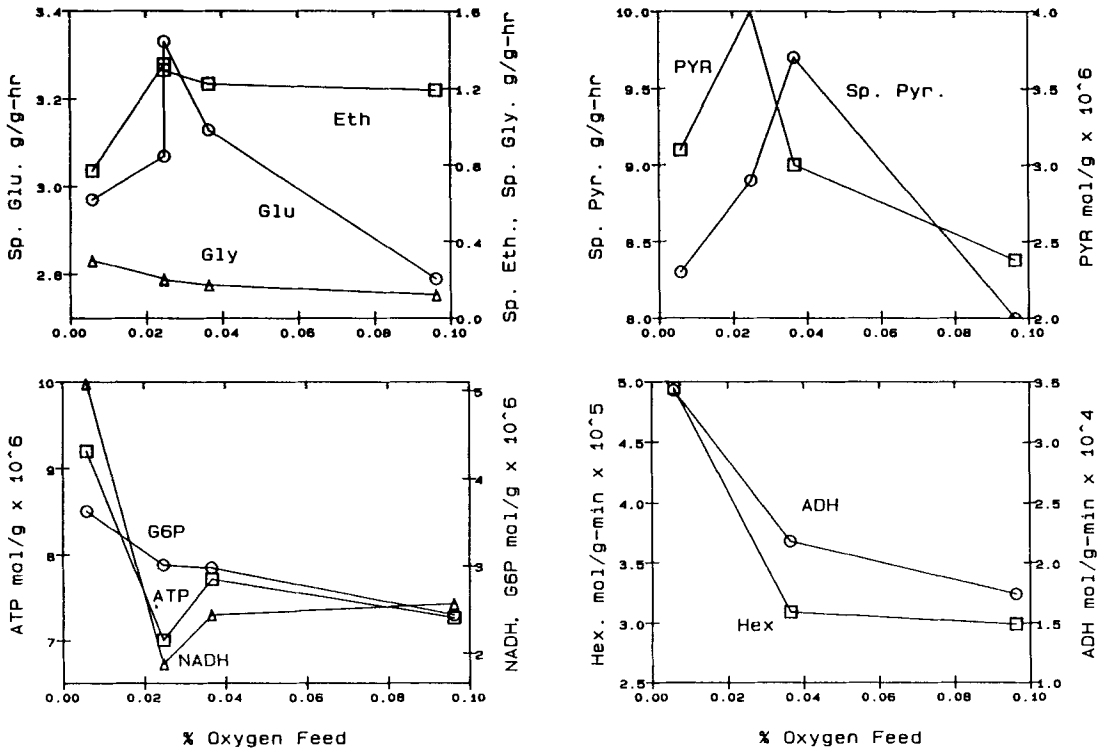

Figure 4. Intracellular enzyme and metabolite assays performed during steady states of run 9. Featured is the transition from 0.024 to 0.0058% feed oxygen in which the specific ethanol productivity decreased significantly.

timal for the pyruvate kinase and phosphoglycerate kinase reactions. A bottleneck at these reactions could account for the observed metabolite pattern. The accumulating species, glucose 6-phosphate and intracellular glycerol, are upstream of the kinases (see Fig. 5). Intracellular pyruvate, the specific pyruvate production rate, and the specific ethanol production rate, which respond to conditions downstream of the kinases, decreased. The threefold increase in the NADH concentration can also be explained. The 3-phosphoglycerate dehydrogenase, an NADH-generating step, is upstream of the kinases, while alcohol dehydrogenase, an NADH-consuming step, is downstream.

It is possible that the increased ATP concentration at the lowest oxygenation steady state also inhibited the allosterically regulated phosphofructokinase reaction. This inhibition may have been possible even though glycerol and NADH, metabolites responding to conditions downstream of PFK, accumulated. Den Hollander et al.,[22] while studying glycolytic regulation in the Pasteur effect, also found retardation of the PFK reaction, despite the accumulation of downstream metabolites. They too concluded that the downstream kinases must also have been involved in the regulation.

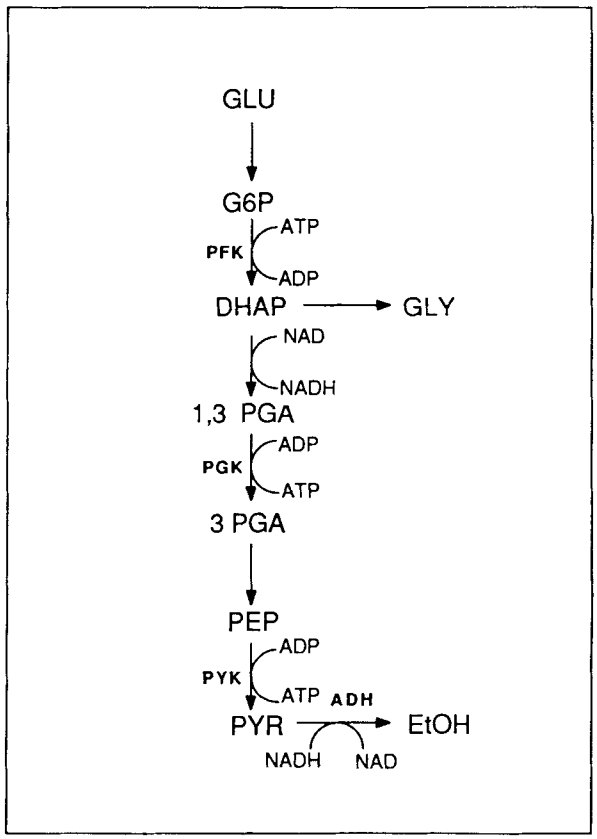

Figure 5. An abbreviation of the glycolytic pathway showing key control points.

ATP Yields and Intracellular ATP Concentrations

The proposed mechanisms for the variations in the metabolic rates and intracellular metabolic patterns are

driven by the changing intracellular ATP concentration. An increasing ATP concentration with decreasing oxygenation resulted in an activation of the glucose transporter and an increased metabolic rate. A further decrease in the oxygenation resulted in the continued accumulation of ATP to the point in which the downstream kinases were inhibited, and the specific ethanol productivity decreased. However, no mechanism has yet been proposed to explain the altered ATP level with changes in the oxygenation.

In addition, as shown in Figure 6 and in Part I, Table IV, wide variations in the ATP growth yield accompanied the metabolic shifts. This necessarily follows from the changes in the amount of ATP supplied by catabolism, despite a constant biosynthetic ATP demand imposed by the fixed dilution rate. These ATP yield variations must now be explained.

First, it is assumed that significant ATP waste reactions such as ATPases and futile cycling exist.[23,24] Such reactions have been proposed to account for the vast discrepancy between measured growth yields and theoretical yields based on biosynthetic and maintenance ATP requirements. The second assumption is that these waste reactions are stimulated by increasing ATP concentration. An example would be an ATPase whose reaction velocity increases with an increasing concentration of its substrate, ATP. Finally, it is assumed that the ATP waste reactions are induced or activated by oxygen in the concentration ranges of this study. Such an assumption is consistent with literature findings. Perleman and Mahler[25] observed that mitochondrial ATPase activity increased upon removal of glucose repression. Glucose derepression of respiration is in many ways analogous to oxygen induction. Rogers and Stewart[26] also found decreased ATP yields and increased maintenance energy requirements upon transition from anaerobic to aerobic conditions. They speculated that more ATP is required to synthesize and maintain mitochondria and structures associated with respiration.

With these assumptions, the increased intracellular ATP concentration with a decreasing oxygen feed rate (Figs. 1 and 4) can be explained. The ATP waste reactions become less active with decreasing oxygenation, allowing for ATP to accumulate. The minimum in the ATP yield (Fig. 6) can be explained, because ATP waste reactions are governed by both the ATP concentration and the oxygen level. The ATP yield decreased when the percent oxygen feed was reduced from 0.38 to 0.024%, because the accumulating ATP concentration affects the ATP waste reactions predominantly in that range. The trend was reversed when the oxygen feed was lowered further to 0.0058%, because the influence of oxygen on ATP waste predominates there.

The behaviors of the ATP yield and the ATP concentration are predicted by theoretical modeling in Part III. The models merely express in mathematical terms the mechanisms affecting catabolism that have already been discussed.

Effect of Antifoam

Another goal of the metabolite assays was to identify the effects of silicone polymer antifoam on yeast metabolism. In the first part of this article series, it was argued that antifoam robs metabolites away from ethanol production towards glycerol production; in the presence of high antifoam concentrations, ethanol productivity was depressed, while glycerol production was stimulated [Part I, Figs. 1,2, and 11]. In Figure 7, the specific glycerol productivity is plotted against the driving force for glycerol efflux across the cell membrane, i.e., the difference between the intracellular and the

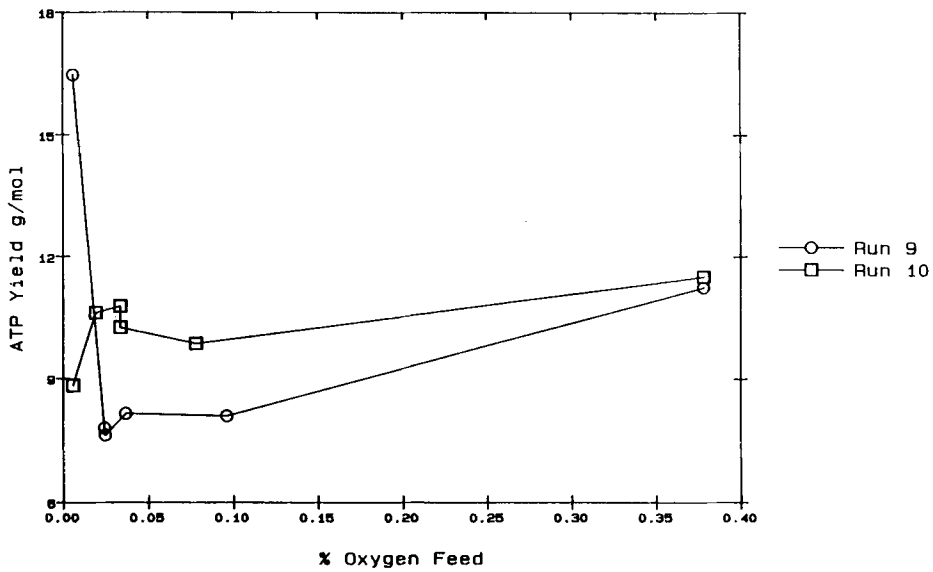

Figure 6. The ATP yield, grams of biomass synthesized per mole of ATP generated in catabolism, in runs 9 and 10.

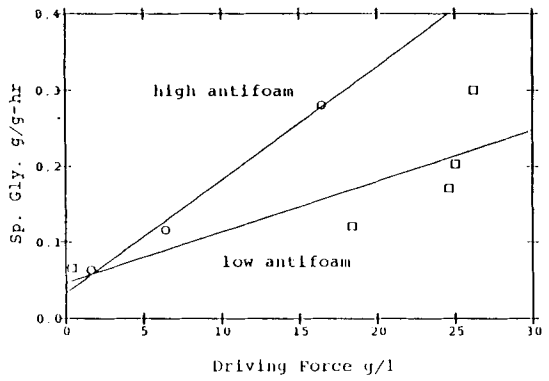

Figure 7. Effect of antifoam on the resistance to glycerol export from the cell. The driving force is the difference between intracellular and extracellular concentrations. Runs 9 and 10 differ mainly in the antifoam concentration in the medium.[1]

extracellular glycerol concentrations. Clearly, the mass transfer resistance across the cell membrane is diminished by the presence of high antifoam levels.

Glycerol production at the expense of ethanol production is likely to create an ATP deficiency in the cell, since glycerol production consumes ATP,[20] while ethanol production generates ATP. The ATP deficiency may have caused the sharp drop in the biomass concentration in the high antifoam culture of run 7 (Part I, Fig. 11) while the drops in the biomass level were avoided in low antifoam cultures (Part I, Figs. 9 and 10). As shown in Figure 8(a), the high antifoam culture of run 10 had consistently lower intracellular ATP levels than the low antifoam culture, run 9. The cause of the lower ATP level is suggested in Figure 8(b) in which the high antifoam culture (run 7) has a diminished specific ethanol productivity. The consequences of the ATP deficiency is demonstrated in Figure 8(c) in which there is a sharp drop in the biomass concentration.

The high antifoam cultures had consistently higher ATP yields, as shown in Figure 6 than low antifoam cultures. This provides further evidence that ATP waste reactions such as ATPases are stimulted by high intracellular ATP concentrations.

A controversy exists in the literature regarding the role of intracellular ethanol in ethanol producing yeast cultures. Reports have been issued of the accumulation of 100–300 g/L intracellular ethanol[6,7] in the early phases of batch culture. However, Dasari et al.[5] have condemned the measurements of these investigators as faulty. The primary complaint was the potential accumulation of huge extracellular ethanol concentrations in dense centrifuged yeast pellets during the delays of the sampling process which would be falsely attributed to intracellular ethanol. Dasari et al.[5] avoided the centrifugation step by cultivating the cell in dense cultures. They concluded that there is little or no difference between the intracellular and extracellular ethanol concentrations. This view is supported by the present data, shown in Figure 9, in which the extracellular ethanol concentration is plotted against their intracellular level.

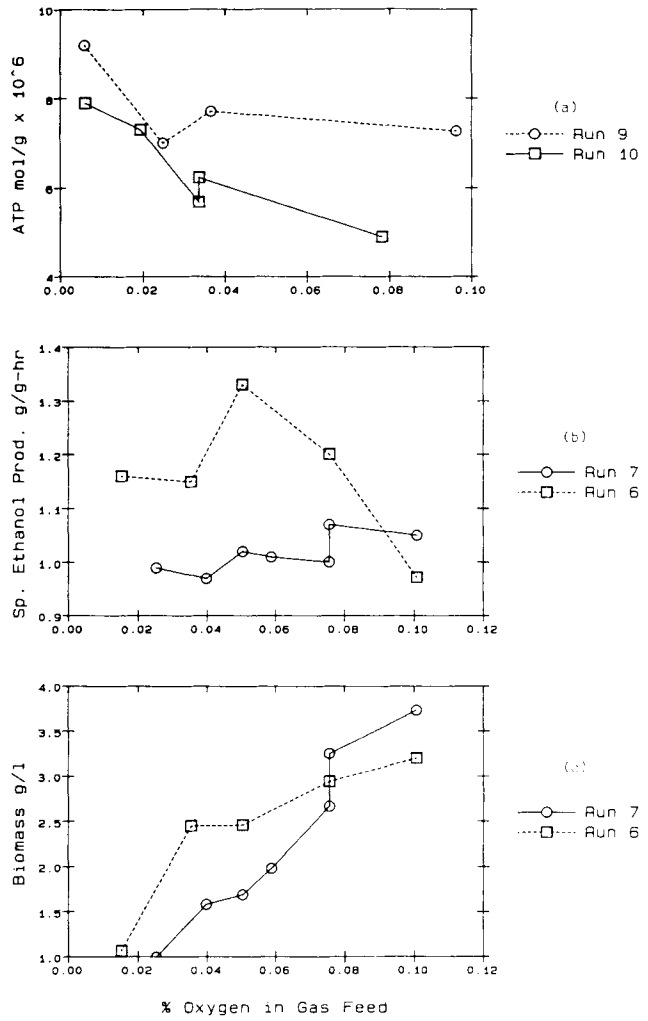

Figure 8. Effect of antifoam on growth and energetics: (a) Intracellular ATP concentration vs. oxygenation in low antifoam run 9 and high antifoam run 10. (b) Specific ethanol productivities in low antifoam run 6 and high-antifoam run 7.[1] (c) Biomass concentration in runs 6 and 7.

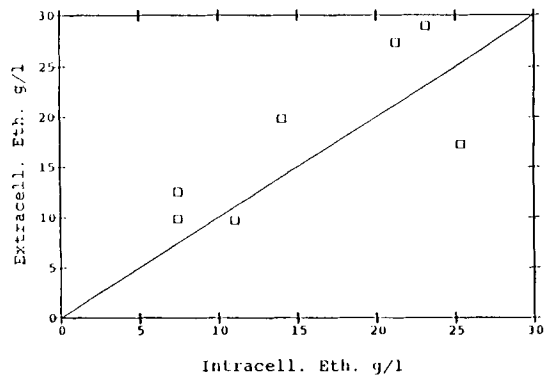

Figure 9. Intracellular versus extracellular ethanol concentrations in runs 9 and 10.

Given the errors inherent in the measurement, no distinction can be made between the concentrations on opposite sides of the cell membrane. It was assumed that the intracellular water volume is 2 mL/g dry wt.[5] Viability in all cases reported exceeded 95%. As a re-

sult, inviability does not enter into consideration of the metabolic phenomena observed.

CONCLUSIONS

The utility of enzyme and intracellular metabolite assays in the elucidation of new metabolic phenomena has been demonstrated. Where metabolic phenomena can be attributed to one or to a few pathways, the assays provide a means to assess rate limiting steps in the phenomenon and the causes of rate limitation.

In this study, the metabolic phenomenon was an acceleration of the metabolic rate with decreasing aeration and the reversal of the intensification with further aeration reduction. Assays of intracellular metabolites spanning the glycolytic pathway implicated the glucose transporter as the rate-limiting step in the metabolic acceleration, and the downstream kinases as the rate-limiting steps in the reversal.

The enzyme and cofactor assays were also instrumental in determining the possible causes of the metabolic changes, as the rate of enzymatic reactions must follow the maximum enzyme activity and its modulation by cofactors as ATP, NADH, etc. The transporter activity was best correlated with the intracellular ATP concentration, which led to the conclusion that ATP is a likely activator of glucose transport. The accumulation of ATP at the lowest oxygenation rate made conditions suboptimal for the downstream kinases, as ADP is reactant and ATP a product of these reactions.

The assays also exposed important metabolic regulations external to the immediate glycolytic pathway. The accumulation of ATP at the lowest oxygen feed rate indicated that the energetic efficiency of growth must change, and that oxygen is a likely cause of the energetic changes. Also, the energetic efficiency was inversely correlated to the ATP concentration, indicating that ATPases and other ATP wasting reactions partially governed the growth efficiency. This conclusion would have been impossible without the ATP concentration measurements to compare to the growth efficiency. In addition, stimulation of glycerol production by antifoam was traced to a possible enhancement of glycerol transport across the cell membrane. To obtain this information, it was necessary to measure the intracellular glycerol concentration, and thus, the driving force for glycerol export. Finally, the ATP measurement fostered speculation that the sudden extinction of the biomass concentration in the fermentor with small environmental changes was caused by a shortage of ATP energy.

In the third part of this article series, an integrated mathematical model is presented embodying the mechanisms and providing explanations for all phenomena observed in this study.

Financial assistance by the National Science Foundation, FYI Grant No. CBT-8514729, with matching funds from Merck & Co., Monsanto Co., and DuPont Co., is gratefully acknowledged. This research was also supported in part by the MIT Biotechnology Process Engineering Center.

References

1. R. Grosz and G. Stephanopoulos, *Biotechnol. and Bioeng.*, **36,** XXX (1990).
2. Y. Nishizawa, I. J. Dunn, and J. R. Bourne, in *Continuous Cultivation of Microorganisms.* Proceedings of the 7th International Symposium, Prague, Czechoslovakia, (1980).
3. D. G. Fraenkel, in *Molecular Biology of the Yeast Saccharomyces: Metabolism and Gene Expression,* J. N. Strathern, E.W. Jones, and J. R. Broach, Eds. (Cold Spring Harbor Laboratory, Cold Spring Harbor, NY, 1982).
4. A. Boituex and B. Hess, in *Biological and Biochemical Oscillators,* B. Chance, E. K. Pye, A. K. Ghosh, and B. Hess, Eds. (Academic, New York, 1973).
5. G. Dasari, E. Keshavarz, M. A. Connor, and N. B. Pamment, *Biotechnol. Lett.,* **7,** 541 (1985).
6. J. M. Navarro, and G. Durand, *Ann. Microbiol. (Inst. Pasteur),* **129b,** 215 (1978).
7. M. Novak, P. Strehaiano, M. Moreno, and G. Goma, *Biotechnol. Bioeng.,* **23,** 201 (1981).
8. R. Grosz, Ph.D. dissertation, California Institute of Technology, Pasadena, CA, 1987.
9. A. G. Chapman and D. E. Atkinson, *Adv. Microb. Physiol.,* **15,** 253 (1977).
10. C. M. M. Franco, J. E. Smith, and D. R. Berry, *J. Gen. Microbiol.,* **130,** 2465 (1984).
11. K. E. Weibel, J. R. Mor, and A. Fiechter, *Anal. Biochem.,* **58,** 208 (1974).
12. W. Bartley and E. S. Polakis, *Biochem. J.,* **99,** 521 (1966).
13. M. J. Beaven, C. Charpentier, and A. H. Rose, *J. Gen. Microbio.,* **128,** 1447 (1982).
14. R. Serrano and G. De La Fuente, *Molec. Cell Biochem.,* **5,** 161 (1974).
15. O. H. Lowry, J.V. Passanneau, and M. K. Rock, *J. Biol. Chem.,* **236,** 2756 (1961).
16. A. Sols, in *Aspects of Yeast Metabolism,* A. K. Mills and H. Krebs, Eds. (Blackwell, Oxford, 1967), p. 47.
17. J. J. Webster and F. R. Leach, *J. Appl. Biochem.,* **66,** 47 (1975).
18. H. A. Bergmeyer, *Methods of Enzymatic Analysis,* 3rd ed. (Verlag Chemie, Deerfield Beach, 1983), Vol. 2.
19. F. C. Womack, and S. P. Colowick, *Proc. Nat. Acad. Sci.,* **76,** 5080 (1979).
20. E. Spoerl, J. P. Williams, and S. H. Benedict, *Biochem. Biophys. Acta,* **298,** 956 (1973).
21. L. F. Bisson and D. G. Fraenkel, *J. Bacteriol.,* **159,** 1013 (1984).
22. J. A. Den Hollander, K. Ugurbil, and R. G. Shulman, *Biochemistry,* **25,** 212 (1986).
23. A. H. Stouthamer, in *Microbial Biochemistry,* J. R. Quayle, Ed. (University Park, Baltimore, 1979), p. 1.
24. R. Lagunas, *Biochem. Biophys. Acta.,* **440,** 661 (1976).
25. P. S. Perlman and H. R. Mahler, *Arch. Biochem. Biophys.,* **162,** 248 (1974).
26. P. J. Rogers and P. R. Stewart, *Arch. Microbiol.,* **99,** 25 (1974).